

## **Supporting Information**

# **Tetrathiafulvalene-Based Helicene Ligand in the Design of Dysprosium Field-Induced Single-Molecule Magnet**

Fabrice Pointillart,<sup>\*a</sup> Jiang-Kun Ou-Yang,<sup>a</sup> Guglielmo Fernandez Garcia,<sup>ab</sup> Vincent Montigaud,<sup>a</sup> Jessica Flores Gonzalez,<sup>a</sup> Rémi Marchal,<sup>a</sup> Ludovic Favereau,<sup>a</sup> Federico Totti,<sup>b</sup> Jeanne Crassous,<sup>\*a</sup> Olivier Cador,<sup>a</sup> Lahcène Ouahab,<sup>a</sup> Boris Le Guennic<sup>\*a</sup>

<sup>a</sup> *Univ Rennes, CNRS, ISCR (Institut des Sciences Chimiques de Rennes) - UMR 6226, 35000 Rennes, France*

<sup>b</sup> *Department of Chemistry « Ugo Schiff » and INSTM RU, University of Florence, 50019 Sesto Fiorentino, Italy.*

Corresponding authors: [fabrice.pointillart@univ-rennes1.fr](mailto:fabrice.pointillart@univ-rennes1.fr), [Boris.leguennic@univ-rennes1.fr](mailto:Boris.leguennic@univ-rennes1.fr), [Jeanne.crassous@univ-rennes1.fr](mailto:Jeanne.crassous@univ-rennes1.fr)

## Experimental Section

### General Procedures and Materials.

The precursors  $\text{Dy}(\text{hfac})_3 \cdot 2\text{H}_2\text{O}$  ( $\text{hfac}^- = 1,1,1,5,5,5$ -hexafluoroacetylacetone anion) and 2-(4,5-(4,5-bis(propylthio)-tetrathiafulvalenyl)-1H-benzimidazol-2-yl)-pyridine were synthesized following previously reported methods.<sup>1,2</sup> All other reagents were purchased from Aldrich Co., Ltd. and used without further purification.

**Synthesis of the ligand 2-[1-[2-methyl[6]helicene]-4,5-[4,5-bis(propylthio)-tetrathiafulvalenyl]-1H-benzimidazol-2-yl]pyridine (L).** 51.9 mg of 2-(4,5-(4,5-bis(propylthio)-tetrathiafulvalenyl)-1H-benzimidazol-2-yl)-pyridine<sup>1</sup> (0.10 mmol) and 21 mg of  $\text{K}_2\text{CO}_3$  (0.15 mmol, 1.5 equiv) were added to 5 mL of DMF, and then the mixture was stirred for 30 min under argon. A solution of 2 mL of DMF containing 30 mg of 2-(Bromomethyl)-[6]-helicene<sup>3</sup> (0.07 mmol, 0.7 equiv) was added, and the resulting mixture was heated at 50 °C. After the mixture had been heated for 2 h, additional  $\text{K}_2\text{CO}_3$  (21 mg, 0.15 mmol, 1.5 equiv) and 2-(Bromomethyl)-[6]-helicene (23 mg, 0.055 mmol, 0.55 equiv) were added. The mixture was stirred and heated overnight. The solvent was evaporated to dryness and the orange residue was washed with water (3 × 50 mL) and extracted with  $\text{CH}_2\text{Cl}_2$ . After evaporation of the  $\text{CH}_2\text{Cl}_2$ , the orange powder was dried in air. Yield: 69 mg (81 %). Anal. Calcd (%) for  $\text{C}_{49}\text{H}_{37}\text{N}_3\text{S}_6$ : C 69.42, H 4.37, N 4.96; found: C 68.99, H 4.47, N 4.89. <sup>1</sup>H-NMR ( $\text{CDCl}_3$ ): 8.28 (m, 1H), 8.23 (m, 1H), 7.95-8.06 (m, 9H), 7.92 (d, 1H), 7.82 (d, 1H), 7.77 (s, 1H), 7.74 (d, 1H), 7.71 (s, 2H), 7.64 (m, 1H), 7.60 (d, 1H), 7.20 (m, 1H), 6.69 (ddd, 1H), 6.68 (s, 2H), 2.85 (dt, 4H), 1.72 (tt, 4H) and 1.06 (dd, 6H).

**[Dy(hfac)<sub>3</sub>(L)]·0.5CH<sub>2</sub>Cl<sub>2</sub>.** 16.4 mg of  $\text{Dy}(\text{hfac})_3 \cdot 2\text{H}_2\text{O}$  (0.02 mmol) were dissolved in 10 mL of  $\text{CH}_2\text{Cl}_2$  and then added to a solution of 10 mL of  $\text{CH}_2\text{Cl}_2$  containing 16.9 mg of L (0.02 mmol). After 20 min of stirring, 40 mL of *n*-hexane were layered at room temperature in the dark. Slow diffusion leads to red single crystals which are suitable for X-ray studies. Yield 25 mg (73 %). Anal. Calcd (%) for  $\text{C}_{64.5}\text{H}_{41}\text{ClDyF}_{18}\text{N}_3\text{O}_6\text{S}_6$ : C 45.90, H 2.43, N 2.49; found: C 45.21, H 2.46 N, 2.39. I.R. (KBr): 2955, 2926, 2870, 2853, 1655, 1574, 1555, 1530, 1508, 1465, 1412, 1255, 1206, 1145, 1102, 1058, 975, 799, 660 and 587 cm<sup>-1</sup>.

**Crystallography.** Single crystal of [Dy(hfac)<sub>3</sub>(L)]·0.5CH<sub>2</sub>Cl<sub>2</sub> was mounted on a APEXIII Bruker-AXS diffractometer for data collection (MoK<sub>α</sub> radiation source,  $\lambda = 0.71073 \text{ \AA}$ ), from the Centre de Diffractométrie (CDIFX), Université de Rennes 1, France. Structures were solved with a direct method using the SHELXT program<sup>4</sup> and refined with a full matrix least-squares method on F<sup>2</sup> using the SHELXL-14/7 program<sup>5</sup>. Crystallographic data are

summarized in Table S1. Complete crystal structure results as a CIF file including bond lengths, angles, and atomic coordinates are deposited as Supporting Information (CCDC number: 1867478).

**Physical Measurements.** The elemental analyses of the compounds were performed at the Centre Régional de Mesures Physiques de l’Ouest, Rennes.  $^1\text{H}$  NMR was recorded on a Bruker Ascend 400 spectrometer. Chemical shifts are reported in parts per million referenced to TMS for  $^1\text{H}$  NMR. Cyclic voltammetry was carried out in  $\text{CH}_2\text{Cl}_2$  solution, containing 0.1 M  $\text{N}(\text{C}_4\text{H}_9)_4\text{PF}_6$  as supporting electrolyte. Voltammograms were recorded at  $100 \text{ mVs}^{-1}$  at a platinum disk electrode. The potentials were measured *versus* a saturated calomel electrode (SCE). The dc and ac magnetic susceptibility measurements were performed on solid polycrystalline samples with a Quantum Design MPMS-XL SQUID magnetometer between 2 and 300 K in applied magnetic field of 0.2 T for temperatures of 2-20 K and 1T for temperatures of 20-300 K. These measurements were all corrected for the diamagnetic contribution as calculated with Pascal’s constants.

**Computational Details.** The atomic positions of the molecule were extracted from the X-ray crystal structures. Only the position of the H and F atoms were optimized on the Y(III) parent complex with the Gaussian 09 (revision D.01) package,<sup>6</sup> employing the PBE0 hybrid functional.<sup>7,8</sup> The “Stuttgart/Dresden” basis sets and effective core potentials were used to describe the yttrium atom,<sup>9</sup> whereas all other atoms were described with the SVP basis sets.<sup>10</sup> Wavefunction-based calculations were carried out on the optimized molecular structure by using the SA-CASSCF/RASSI-SO approach, as implemented in the MOLCAS quantum chemistry package (versions 8.0).<sup>11</sup> In this approach, the relativistic effects are treated in two steps on the basis of the Douglas–Kroll Hamiltonian. First, the scalar terms were included in the basis-set generation and were used to determine the spin-free wavefunctions and energies in the complete active space self-consistent field (CASSCF) method.<sup>12</sup> Next, spin-orbit coupling was added within the restricted-active-space state-interaction (RASSI-SO) method, which uses the spin-free wavefunctions as basis states.<sup>13,14</sup> The resulting wavefunctions and energies are used to compute the magnetic properties and g-tensors of the lowest states from the energy spectrum by using the pseudospin  $S = 1/2$  formalism in the SINGLE-ANISO routine.<sup>15,16</sup> Cholesky decomposition of the bielectronic integrals was employed to save disk space and speed-up the calculations.<sup>17</sup> The active space of the self-consistent field (CASSCF) method consisted of the nine 4f electrons of the  $\text{Dy}^{\text{III}}$  ion spanning the seven 4f orbitals, i.e. CAS(9,7)SCF. State-averaged CASSCF calculations were performed for all of the sextets (21

roots), all of the quadruplets (224 roots), and 300 out of the 490 doublets (due to software limitations) of the Dy<sup>III</sup> ion. 21 sextets, 128 quadruplets, and 107 doublets were mixed through spin–orbit coupling in RASSI-SO. All atoms were described by ANO-RCC basis sets.<sup>18-20</sup> The following contractions were used: [8s7p4d3f2g1h] for Dy, [4s3p2d] for the O and N atoms directly coordinated to Dy, [4s3p1d] for C atoms in the second coordination sphere, [3s2p] for the C, F and S atoms and other O and N atoms, and [2s] for the H atoms.

To give more insights on the orientation of the magnetic axis, the molecular electrostatic potential is calculated from the ab-initio LoProp charge analysis<sup>21</sup> following Eq. 1,

$$V(r_i) = \sum_i^N \frac{q_i}{|r_i - r|} + \frac{p_i \cdot r_i}{|r_i - r|^3} + \frac{r_i \cdot (Q_i \times r_i)}{|r_i - r|^5} \quad (\text{eq. 1})$$

where  $q_i$ ,  $p_i$ ,  $Q_i$  are respectively the monopole, dipole and quadrupole moments of the  $i$ -th atom. The resulting molecular electrostatic potential is mapped and represented using the home-made CAMMEL code (CAlculated Molecular Multipolar ELectrostatics). The potential is drawn on a sphere defined by the user around the central lanthanide ion, for a given state (ground state in this case). For a clearer representation of the potential, the intensity can be directly related to both the color (red = high potential and blue = low potential) and the height of the irregularities.

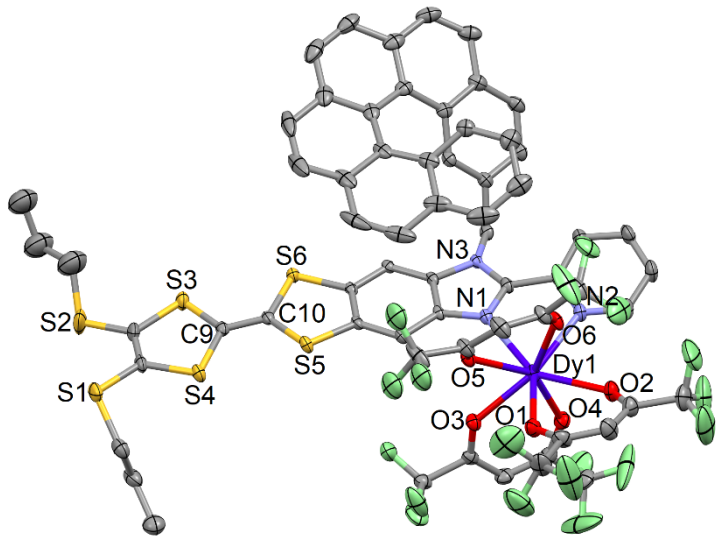


**Figure S1.** ORTEP view of  $[Dy(hfac)_3(L)] \cdot 0.5CH_2Cl_2$  in  $CH_2Cl_2$ . Thermal ellipsoids are drawn at 30% probability. Hydrogen atoms are omitted for clarity.

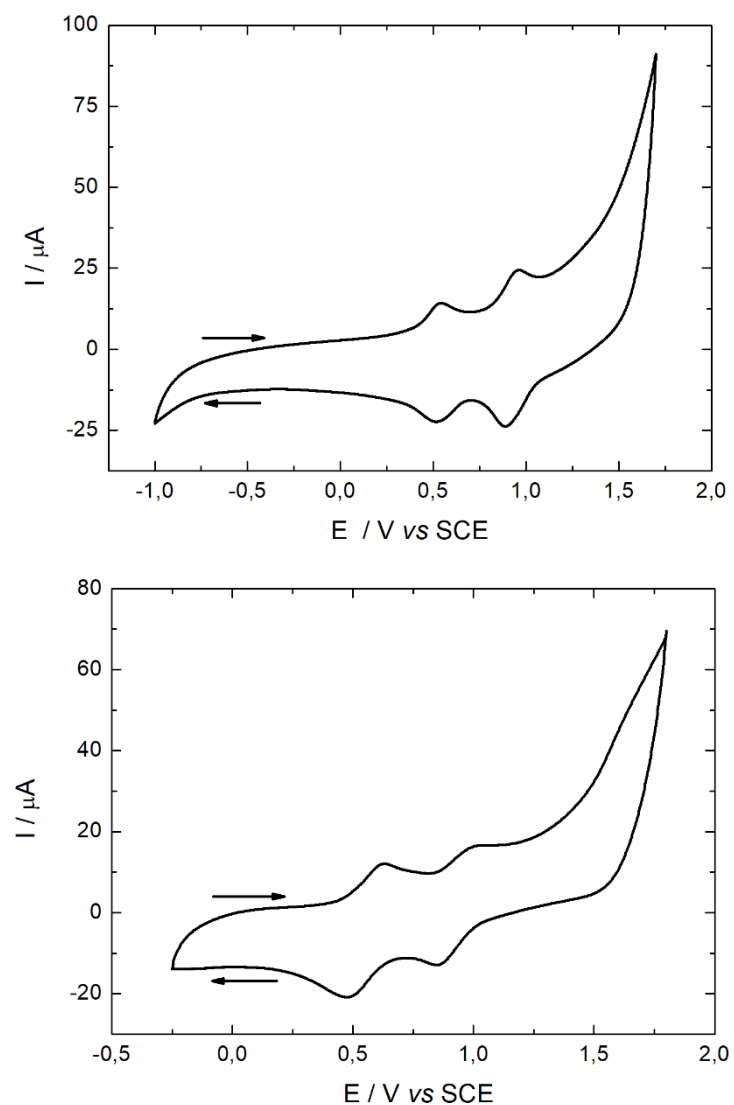


**Figure S2.** Cyclic voltammograms of **L** (top) and  $[\text{Dy}(\text{hfac})_3(\mathbf{L})] \cdot 0.5\text{CH}_2\text{Cl}_2$  (bottom) in  $\text{CH}_2\text{Cl}_2$  at a scan rate of  $100 \text{ mV} \cdot \text{s}^{-1}$ . The potentials were measured *vs.* a saturated calomel electrode (SCE) with Pt wires as working and counter electrodes.

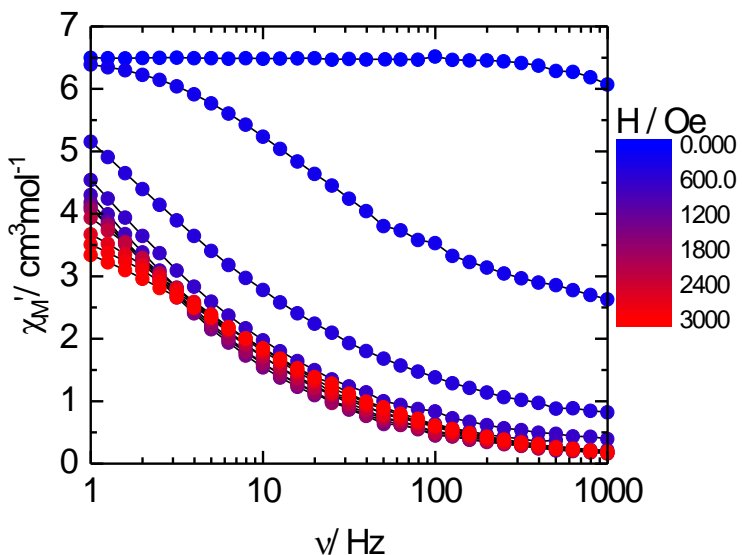


**Figure S3.** Frequency dependence of  $\chi_M'$  of  $[\text{Dy(hfac)}_3(\text{L})] \cdot 0.5\text{CH}_2\text{Cl}_2$  at 2 K between 0 and 3000 Oe.

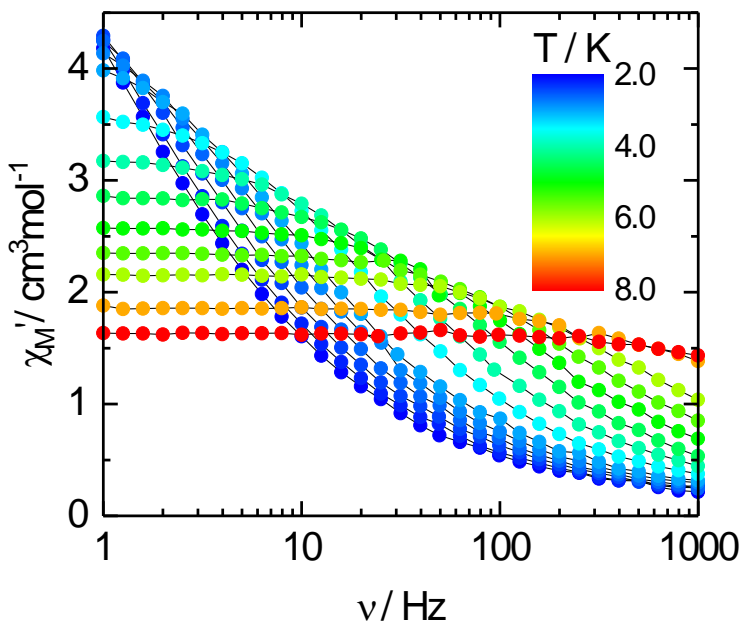


**Figure S4.** Frequency dependence of  $\chi_M'$  of  $[\text{Dy(hfac)}_3(\text{L})] \cdot 0.5\text{CH}_2\text{Cl}_2$  between 2 and 8 K at 1000 Oe.

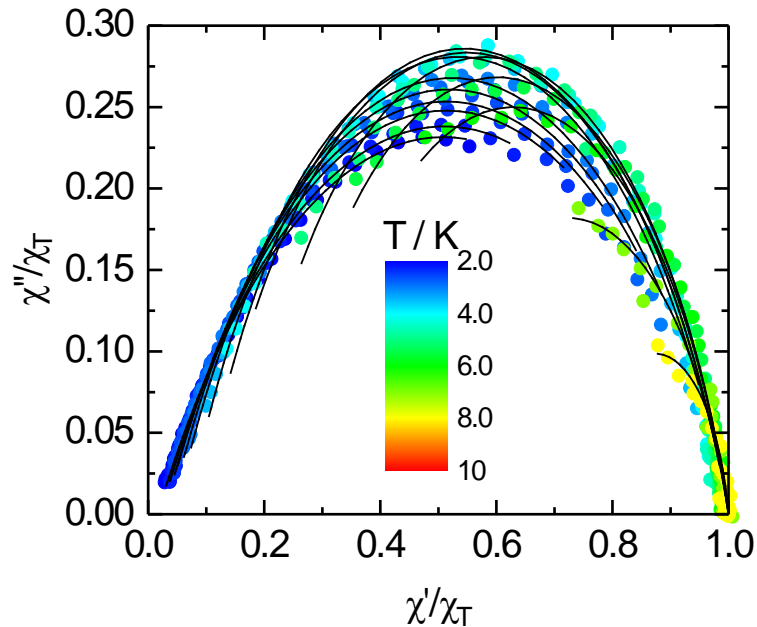


**Figure S5.** Normalized Cole-Cole plots at several temperatures between 2 and 8 K.

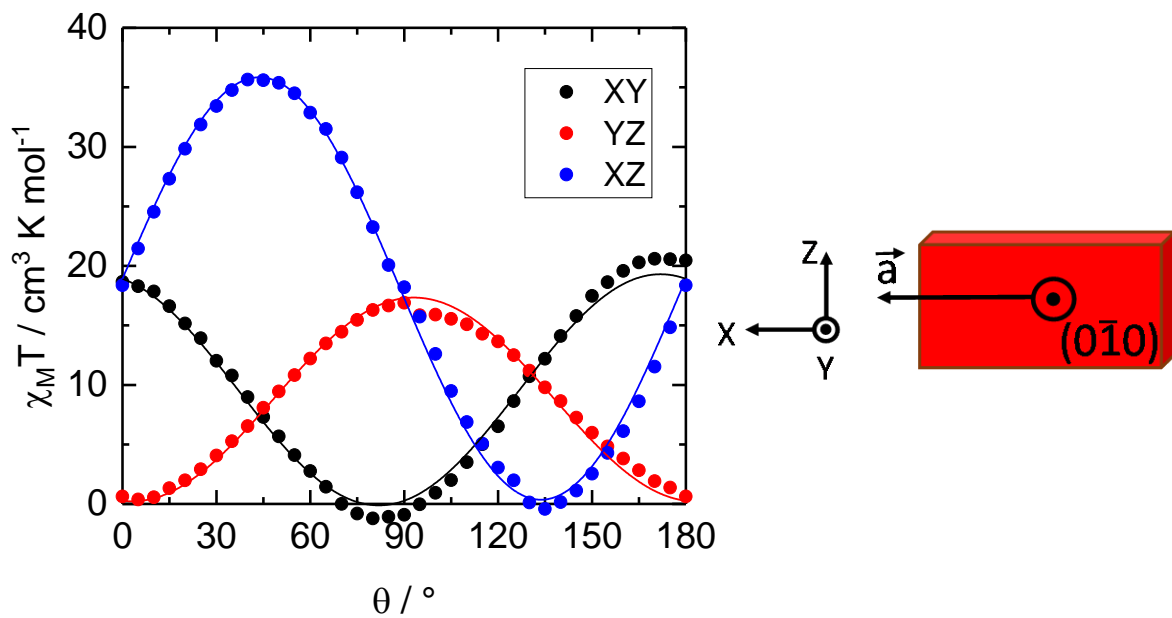


**Figure S6.** (left) Angular dependence of  $\chi_M T$  of a single crystal rotating in three perpendicular planes with  $H = 1$  kOe at 2 K. Full lines are best-fitted curves (right) orientation of the single crystal within the XYZ crystal reference frame.

Susceptibility tensor in the crystal frame (XYZ):

$$\chi_M T = \begin{pmatrix} 18.91129 & -2.71166 & 17.72671 \\ -2.71166 & 0.26866 & -0.92697 \\ 17.72671 & -0.92697 & 17.28682 \end{pmatrix} \text{cm}^3 \text{K mol}^{-1}$$

Principal values and direction of the susceptibility tensor in the XYZ crystal frame:

$$\chi_{xx} T \begin{pmatrix} 0.498 \\ 0.744 \\ -0.445 \end{pmatrix} = -0.991, \quad \chi_{yy} T \begin{pmatrix} -0.479 \\ 0.664 \\ -0.445 \end{pmatrix} = 1.424, \quad \chi_{zz} T \begin{pmatrix} 0.723 \\ -0.073 \\ 0.687 \end{pmatrix} = 36.034 \text{ cm}^3 \text{K mol}^{-1}$$

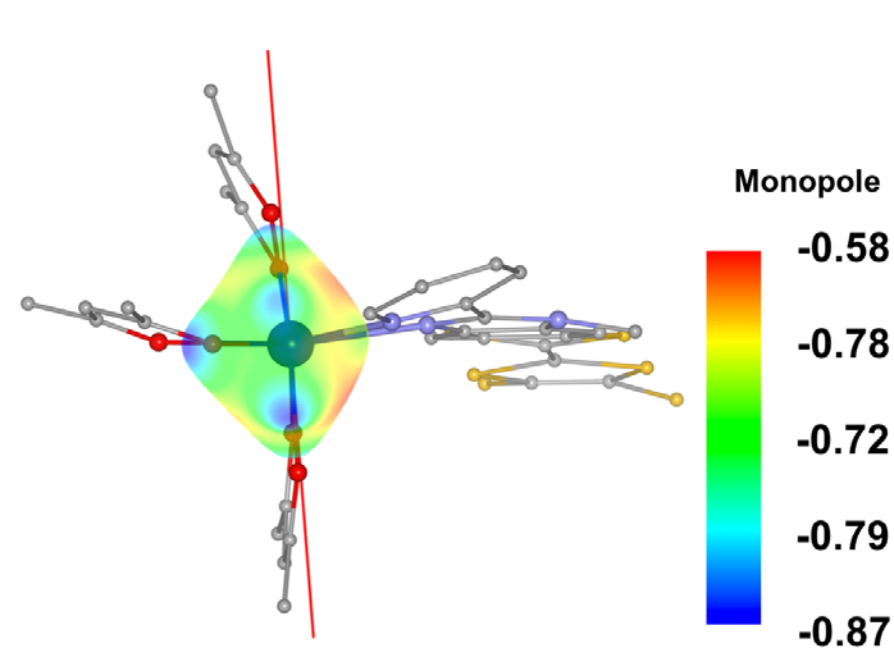


**Figure S7.** Representation of the monopole (charge) contribution to the total electrostatic potential of the ground state. The red line corresponds to the orientation of the ground state magnetic axis. The helicene moiety and a part of the TTF ligand are omitted for the sake of clarity.

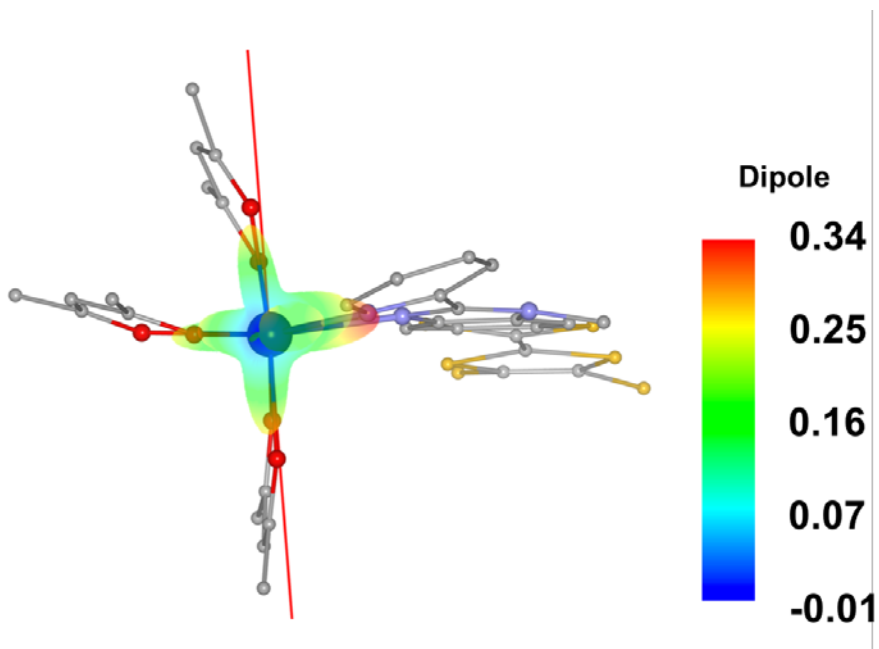


**Figure S8.** Representation of the dipolar contribution to the total electrostatic potential, for the ground state. The red line corresponds to the orientation of the ground state magnetic axis. The helicene moiety and a part of the TTF ligand are omitted for the sake of clarity.

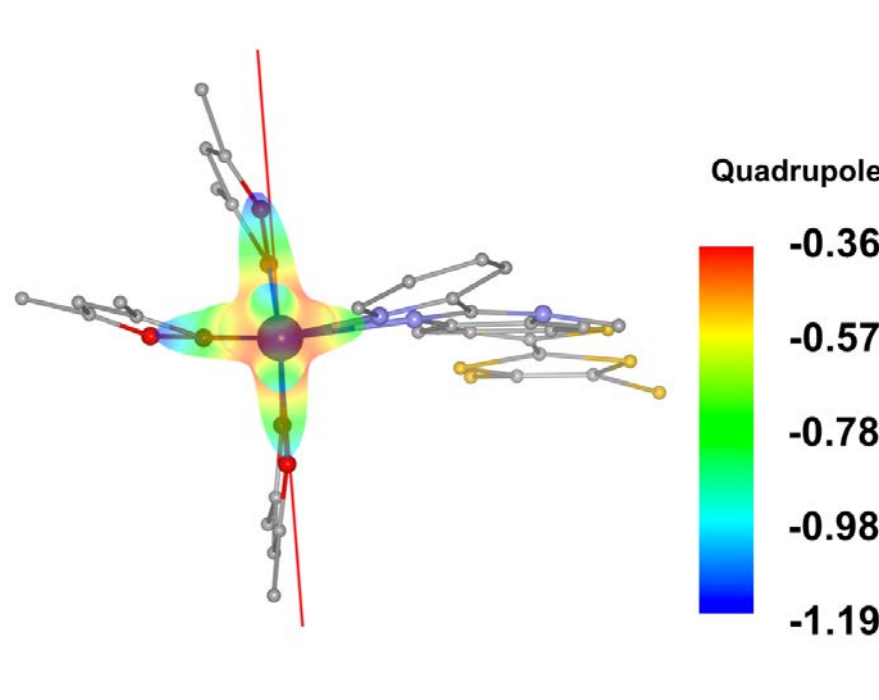


**Figure S9.** Representation of the quadrupolar contribution to the total electrostatic potential, for the ground state. The red line corresponds to the orientation of the ground state magnetic axis. The helicene moiety and a part of the TTF ligand are omitted for the sake of clarity.

**Table S1.** Crystallographic data for  $[\text{Dy}(\text{hfac})_3(\mathbf{L})]\cdot\text{CH}_2\text{Cl}_2$ .

Compound	$[\text{Dy}(\text{hfac})_3(\mathbf{L})]\cdot0.5\text{CH}_2\text{Cl}_2$
Formula	$\text{C}_{64.5}\text{H}_{41}\text{ClDyF}_{18}\text{N}_3\text{O}_6\text{S}_6$
$M / \text{g.mol}^{-1}$	1686.3
Crystal system	Triclinic
Space group	P-1 ( $N^{\circ}2$ )
Cell parameters	$a = 13.3879(14) \text{\AA}$ $b = 16.1474(16) \text{\AA}$ $c = 17.1709(14) \text{\AA}$ $\alpha = 106.141(3)^\circ$ $\beta = 96.476(3)^\circ$ $\gamma = 105.975(6)^\circ$
Volume / $\text{\AA}^3$	3355.2(6)
Cell formula units	2
$T / \text{K}$	150 (2)
Diffraction reflection	$5.96 \leq 2\theta \leq 54.97$
$\rho_{\text{calc}}, \text{g.cm}^{-3}$	1.669
$\mu, \text{mm}^{-1}$	1.444
Number of reflections	80128
Independent reflections	15366
$Fo^2 > 2\sigma(Fo)^2$	11658
Number of variables	896
$R_{\text{int}}, R_1, wR_2$	0.0503, 0.0577, 0.1392

**Table S2.** First three solutions of the SHAPE analysis.

Triangular dodecahedron ( $D_{2d}$ )	Biaugmented trigonal prism ( $C_{2v}$ )	Square antiprism ( $D_{4d}$ )
0.586	2.223	2.799

**Table S3.** Oxidation potentials (V vs SCE,  $n\text{Bu}_4\text{NPF}_6$ , 0.1 M in  $\text{CH}_2\text{Cl}_2$  at 100  $\text{mV.s}^{-1}$ ) of the ligand **L** and complex  $[\text{Dy}(\text{hfac})_3(\mathbf{L})]\cdot0.5\text{CH}_2\text{Cl}_2$ .

	$E^{1/2} / \text{V}$		$E^{2/2} / \text{V}$	
	${}^{\text{ox}}E^1$	${}^{\text{red}}E^1$	${}^{\text{ox}}E^2$	${}^{\text{red}}E^2$
<b>L</b>	0.54	0.51	0.96	0.89
$[\text{Dy}(\text{hfac})_3(\mathbf{L})]\cdot\text{CH}_2\text{Cl}_2$	0.63	0.47	1.03	0.85

$$* E^n_{1/2} = ({}^{\text{ox}}E_n + {}^{\text{red}}E_n)/2 \quad (n = 1, 2)$$

**Table S4.** Best fitted parameters ( $\chi_T$ ,  $\chi_S$ ,  $\tau$  and  $\alpha$ ) with the extended Debye model for compound [Dy(hfac)<sub>3</sub>(L)]·0.5CH<sub>2</sub>Cl<sub>2</sub> at 1000 Oe in the temperature range 2-8 K.

T / K	$\chi_T$ / cm <sup>3</sup> mol <sup>-1</sup>	$\chi_S$ / cm <sup>3</sup> mol <sup>-1</sup>	$\alpha$	$\tau$ / s	R <sup>2</sup>
2	7.55121	0.12212	0.43976	0.79003	0.99977
2.2	6.75791	0.14142	0.42347	0.51939	0.99970
2.4	5.93307	0.15984	0.40008	0.30772	0.99951
2.6	5.38396	0.15533	0.38749	0.19871	0.99939
2.8	4.90730	0.18176	0.36789	0.13135	0.99938
3	4.50810	0.20940	0.34833	0.09037	0.99938
3.5	3.77262	0.25549	0.30957	0.03971	0.99955
4	3.28731	0.29259	0.28631	0.02001	0.99943
4.5	2.93220	0.28986	0.28498	0.01053	0.99928
5	2.61366	0.41528	0.25054	0.00644	0.99963
5.5	2.37825	0.48784	0.24399	0.00392	0.99970
6	2.17717	0.56222	0.24495	0.00232	0.99978
7	1.86771	0.83847	0.25732	0.00095	0.99987
8	1.63281	1.22456	0.15046	0.00097	0.99987

**Table S5.** g tensor and energy splitting of the multiplet ground state of  $[\text{Dy}(\text{hfac})_3(\text{L})] \cdot 0.5\text{CH}_2\text{Cl}_2$ .

	E (cm <sup>-1</sup> )	g <sub>x</sub>	g <sub>y</sub>	g <sub>z</sub>	Wavefunction composition
1	0.00	0.09	0.22	19.09	0.88  ±15/2> + 0.10  ±11/2>
2	56.91	0.59	0.75	18.27	0.40  ±1/2> + 0.30  ±3/2> + 0.17  ±7/2> + 0.04  ± 13/2>
3	110.78	3.79	4.75	11.29	0.50  ±13/2> + 0.26  ±9/2> + 0.07  ±3/2> + 0.06  ± 5/2>
4	160.10	2.91	4.57	10.20	0.38  ±7/2> + 0.15  ±11/2> + 0.13  ±5/2> + 0.10  ± 1/2>
5	203.47	0.57	1.59	16.24	0.38  ±5/2> + 0.21  ±3/2> + 0.15  ±1/2> + 0.12  ± 7/2>
6	243.59	0.56	0.98	16.42	0.29  ±3/2> + 0.27  ±1/2> + 0.13  ±5/2> + 0.11  ± 11/2>
7	288.78	0.10	0.19	18.94	0.27  ±9/2> + 0.26  ±11/2> + 0.18  ±7/2> + 0.13  ± 13/2>
8	332.20	0.00	0.09	18.95	0.30  ±9/2> + 0.30  ±11/2> + 0.16  ±7/2> + 0.13  ± 13/2>

## References

- (1) Wu, J.; Dupont, N.; Liu, S.-X.; Neels, A.; Hauser, A.; Decurtins, S. Imidazole-Annulated Tetrathiafulvalene Exhibiting pH-Tunable Intramolecular Charge Transfer and Redox Properties. *Chem. Asian J.* **2009**, *4*, 392-399.
- (2) Richardson, M. F.; Wagner, W. F.; Sands, D. E. Rare-earth trishexafluoroacetylacetones and related compounds. *J. Inorg. Nucl. Chem.* **1968**, *30*, 1275-1289.
- (3) Storch, J.; Zadny, J.; Strasak, T.; Kubala, M.; Sykora, J.; Dusek, M.; Cirkva, V.; Matejka, P.; Krbal, M.; Vacek. J. Synthesis and Characterization of a Helicene-Based Imidazolium Salt and Its Application in Organic Molecular Electronics. *Chem. Eur. J.* **2015**, *21*, 2343-2347.
- (4) Lunghi, A.; Totti, F.; Sanvito, S.; Sessoli, R. Intra-molecular origin of the spin-phonon coupling in slow-relaxing molecular magnets. *Chem. Sci.*, **2017**, *8*, 6051–6059.
- (5) Sheldrick, G. M. Crystal structure refinement with SHELXL. *Acta Crystallogr. Sect. C* **2015**, *71*, 3-8.
- (6) Gaussian 09, Revision D.01, Frisch, M. J.; Trucks, G. W.; Schlegel, H. B.; Scuseria, G. E.; Robb, M. A.; Cheeseman, J. R.; Scalmani, G.; Barone, V.; Petersson, G. A.; Nakatsuji, H.; Li, X.; Caricato, M.; Marenich, A.; Bloino, J.; Janesko, B. G.; Gomperts, R.; Mennucci, B.;

- Hratchian, H. P.; Ortiz, J. V.; Izmaylov, A. F.; Sonnenberg, J. L.; Williams-Young, D.; Ding, F.; Lipparini, F.; Egidi, F.; Goings, J.; Peng, B.; Petrone, A.; Henderson, T.; Ranasinghe, D.; Zakrzewski, V. G.; Gao, J.; Rega, N.; Zheng, G.; Liang, W.; Hada, M.; Ehara, M.; Toyota, K.; Fukuda, R.; Hasegawa, J.; Ishida, M.; Nakajima, T.; Honda, Y.; Kitao, O.; Nakai, H.; Vreven, T.; Throssell, K.; Montgomery, Jr J. A.; Peralta, J. E.; Ogliaro, F.; Bearpark, M.; Heyd, J. J.; Brothers, E.; Kudin, K. N.; Staroverov, V. N.; Keith, T.; Kobayashi, R.; Normand, J.; Raghavachari, K.; Rendell, A.; Burant, J. C.; Iyengar, S. S.; Tomasi, J.; Cossi, M.; Millam, J. M.; Klene, M.; Adamo, C.; Cammi, R.; Ochterski, J. W.; Martin, R. L.; Morokuma, K.; Farkas, O.; Foresman, J. B. and Fox, D. J. Gaussian, Inc., Wallingford CT, 2016.
- (7) Perdew, J. P.; Burke, K.; Ernzerhof, M. Generalized Gradient Approximation Made Simple. *Phys. Rev. Lett.* **1996**, *77*, 3865–3868.
- (8) Adamo, C.; Barone, V. Toward reliable density functional methods without adjustable parameters: The PBE0 model. *J. Chem. Phys.* **1999**, *110*, 6158–6170.
- (9) Dolg, M.; Stoll, H.; Preuss, H. A combination of quasirelativistic pseudopotential and ligand field calculations for lanthanoid compounds. *Theor. Chim. Acta* **1993**, *85*, 441–450.
- (10) Weigend, F.; Ahlrichs, R. Balanced basis sets of split valence, triple zeta valence and quadruple zeta valence quality for H to Rn: Design and assessment of accuracy. *Phys. Chem. Chem. Phys.* **2005**, *7*, 3297–3305.
- (11) Aquilante, F.; Autschbach, J.; Carlson, R. K.; Chibotaru, L. F.; Delcey, M. G.; De Vico, L.; Galván, I. F.; Ferré, N.; Frutos, L. M.; Gagliardi, L.; Garavelli, M.; Giussani, A.; Hoyer, C. E.; Manni, G. L.; Lischka, H.; Ma, D. X.; Malmqvist, P.; Müller, T.; Nenov, A.; Olivucci, M.; Pedersen, T. B.; Peng, D. L.; Plasser, F.; Pritchard, B.; Reiher, M.; Rivalta, I.; Schapiro, I.; Segarra-Martí, J.; Stenrup, M.; Truhlar, D. G.; Ungur, L.; Valentini, A.; Vancoillie, S.; Veryazov, V.; Vysotskiy, V. P.; Weingart, O.; Zapata, F.; Lindh, R. Molcas 8: New Capabilities for Multiconfigurational Quantum Chemical Calculations Across the Periodic Table. *J. Comput. Chem.* **2016**, *37*, 506–541.
- (12) Roos, B. O.; Taylor, P. R.; Siegbahn, P. E. M. A complete active space SCF method (CASSCF) using a density matrix formulated super-CI approach. *Chem. Phys.* **1980**, *48*, 157–288.
- (13) Malmqvist, P. A.; Roos, B. O.; Schimmelpfennig, B. The restricted active space (RAS) state interaction approach with spin-orbit coupling. *Chem. Phys. Lett.* **2002**, *357*, 230–240.
- (14) Malmqvist, P. A.; Roos, B. O. The CASSCF state interaction method. *Chem. Phys. Lett.* **1989**, *155*, 189–194.

- (15) Chibotaru, L. F.; Ungur, L. *Ab initio* calculation of anisotropic magnetic properties of complexes. I. Unique definition of pseudospin Hamiltonians and their derivation. *J. Chem. Phys.* **2012**, *137*, 064112–064122.
- (16) Chibotaru, L. F.; Ungur, L.; Soncini, A. The Origin of Nonmagnetic Kramers Doublets in the Ground State of Dysprosium Triangles: Evidence for a Toroidal Magnetic Moment. *Angew. Chem., Int. Ed.* **2008**, *47*, 4126–4129.
- (17) Aquilante, F.; Malmqvist, P.-A.; Pedersen, T.-B.; Ghosh, A.; Roos, B. O. Cholesky Decomposition-Based Multiconfiguration Second-Order Perturbation Theory (CD-CASPT2): Application to the Spin-State Energetics of Co<sup>III</sup>(diiminato)(NPh). *J. Chem. Theory Comput.* **2008**, *4*, 694–702.
- (18) Roos, B. O.; Lindh, R.; Malmqvist, P.-A.; Veryazov, V.; Widmark, P.-O. Main Group Atoms and Dimers Studied with a New Relativistic ANO Basis Set. *J. Phys. Chem. A* **2004**, *108*, 2851–2858.
- (19) Roos, B. O.; Lindh, R.; Malmqvist, P.-A.; Veryazov, V.; Widmark, P.-O. New Relativistic ANO Basis Sets for Transition Metal Atoms. *J. Phys. Chem. A* **2005**, *109*, 6575–6579.
- (20) Roos, B. O.; Lindh, R.; Malmqvist, P.-A.; Veryazov, V.; Widmark, P.-O.; Borin, A.-C. New relativistic Atomic Natural Orbital Basis Sets for lanthanide Atoms with Applications to the Ce Diatom and LuF<sub>3</sub>. *J. Phys. Chem. A* **2008**, *112*, 11431–11435.
- (21) Laura, G.; Roland, L.; Gunnar, K. Local properties of quantum chemical systems: The LoProp approach. *J. Chem. Phys.* **2004**, *121*, 4494.